Semiconductor Optoelectronics
ISSN: 1001-5868

EFFICIENCY AND DURABILITY OF THIN-FILM P-TYPE HYDROGENATED AMORPHOUS SILICON (a − Si: H) SOLAR CELLS

Santosh Kumar Srivastava, Jitendra Singh
Assistant Professor, Department of Physics, Shri Lal Bahadur Shastri Degree College Gonda, Uttar Pradesh,
Professor, Department of Physics, Shri Lal Bahadur Shastri Degree College, Gonda, Uttar Pradesh,

Abstract

a − Si: H is a kind of amorphous silicon in which the silicon atoms are not arranged in a Bravais lattice. In 1969, while there was a revival of interest in non- a − Si: H, the year 1969 also saw the manufacturing of a − Si: H. A lot of studies are being done currently on the inefficient but low-cost possibility of using a-Si: H as the active substance in solar cells. In the study, they have reported the outcomes of a numerical implementation of an a − Si: H solar cell produced by the Plasma-Enhanced Chemical Vapour Deposition (PECVD) method, and the thicknesses of the process were determined using Atomic Force Microscopy (AFM). They also investigate the impact that the thickness of the a − Si: H p-layer has on the open-circuit voltage (V_{oc}), Short-circuit current (J_{sc}), fill factor (FF), and conversion efficiency (E_{ff}) characteristics of the Solar cell. The hydrogen dilution ratio that is used during the process of deposition is one of the parameters which can have an impact on the efficiency of Solar cells. Solar cell efficiency could be improved by 5.6% due to B2's effects. In addition, the thickness of the p-layer was changed between 400 along with 800 nano-meters. A modification in thickness results in a 5.91% development in the E_{ff} of the Solar cell.

Keywords: Solar Cells, Amorphous silicon, Atomic Force Microscopy, PECVD, semiconductor

1. Introduction

The p-n junction is the simplest semiconductor junction and is used to segregate photogenerated charge carriers in Solar cells by providing an interface between the p-type and n-type regions of a single semiconductor. The capacity to control the material's conductivity by doping is a hallmark of semiconductors and must be shown before the material can be considered for use in solar cells. This was the situation with amorphous Silicon (a-Si). In 1965, the first a-Si layers were described as films of silicon from silane formed in a radio frequency glow discharge. It wasn't until Dundee University's Spear and Lacombe demonstrated that a-Si could be doped type and p-type by using phosphine or diborane in the glow discharge gas mixture that it was generally believed that a − Si exhibited semiconducting qualities [1].

This discovery was all the more remarkable since it disproved the widely held notion that a − Si could not be doped. There was a delay in recognizing the significance of hydrogen to the

newly created $a-Si$ doped films. $a-Si$ is a silicon–hydrogen alloy that is particularly well suited for doping in electrical applications. Electronics grade amorphous silicon is known as $a-Si:H$.

To successfully collect the photogenerated charge carriers, $a-Si:H$ solar cells [2] employ a $p-i-n$ or $n-i-p$ diode structure composed of substantially unreliable n and p-doped layers and an intrinsic $a-Si:H$ layer as a light absorption layer. There has been a lot of interest in the manufacturing of $a-Si:H$ substrate-type $(n-i-p)$ thin film solar cells on ambiguous and flexible substrates like metal films or plastic films for the variability of applications, with the construction of Photovoltaic (PV) equipped buildings and the provision of energy for mobile devices, sensors, and displays [3-4].

PECVD is used for much of the manufacturing process because it makes it simple to perform the hydrogenation and doping processes on a thin layer. The deposition parameters can be controlled into extremely broad changes employing PECVD which results in varied optical and electronic properties on $a-Si:H$ thin layer. As the PECVD device production technology can generate sufficient quantities of solar cells to meet the demands of large-scale industry, it is frequently employed. V_{oc}, J_{sc}, FF, and E_{ff} were some of the cell performances compared through simulation.

The study follows the following Section: In Section 2, the authors provide a literature assessment efficiency and durability of thin-film p-type $a-Si:H$ Solar Cells. In Section 3, the authors survey prior studies, and Section 4, states the issue and provide a solution. The study materials and methods are presented in Section 5. The latter section is the basis for the anticipated findings presented in Section 6. The report then draws a final judgment and makes recommendations for further study in section 7.

1.1 Solar Cells

In 1839, Alexandre-Edmond Becquerel was the first person to notice the solar effect [5]. Cells that absorb sunlight and convert it directly into energy are known as solar cells or PV cells. In 1946, Russel Ohl developed the initial silicon solar cell, which is considered to be the first true modern solar cell [5-6]. Thin silicon wafers were employed in the first generation of solar cells, which transformed sunlight into electricity. As can be seen in Figure 1, contemporary solar cells operate based on the formation of electron holes in all cells, which consists of two layers (p-type and n-type materials) of semiconductor material.

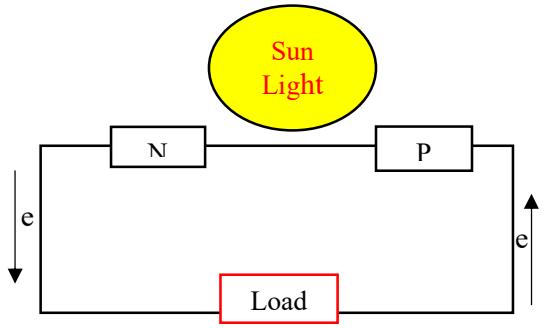

Figure 1: Semiconductor p-n junction solar cell [7].

When a photon with sufficient energy encroaches on the p-type and n-type junctions in the

structure, an electron is released and goes from one layer to another by acquiring energy from the affecting photon. Electrical power is produced as a result of this because it simultaneously generates an electron and a hole [8]. Silicon (in single crystal, multi-crystalline, and amorphous forms) [9-11], cadmium-telluride (Cd-Te) [12], copper-indium-gallium-selenide (CIGS) [13], and copper-indium-gallium-sulfide are only a few of the numerous substances used in solar cells [14]. Several types of PV cells are addressed in the following sections according to the materials they are made from (also shown in Figure 2) [15-17].

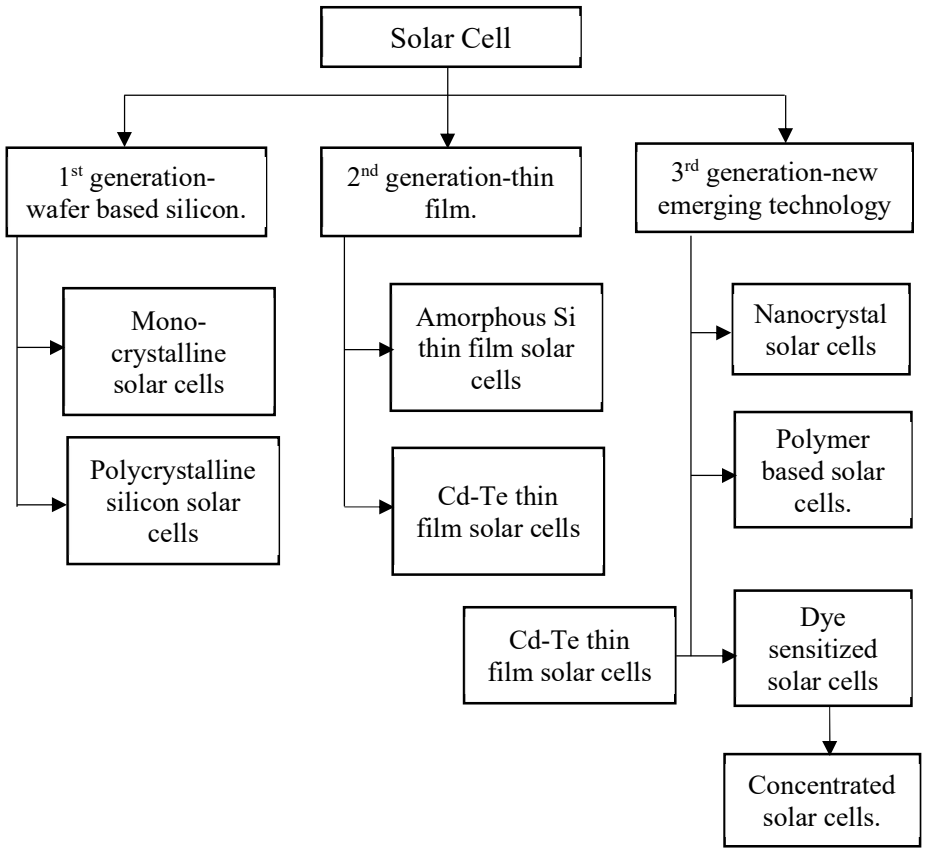

Figure 2: Solar cell kinds and development trends [18-21].

i. First Generation Solar Cell-Wafer Based

The initial generations of Solar cells are manufactured on silicon wafers. In terms of power efficiency, it is both the eldest and most promising technology. Technologies based on silicon wafers can be broken down even further into two subtypes:

- Single/ Mono-crystalline silicon (Mono c-Si) solar cell.
- Poly/Multi-crystalline silicon (Multi c-Si) solar cell.

Single/Mono c-Si Solar cell:

Mono c-Si, commonly referred to as single-crystal silicon, is the primary component of silicon chips, which are the building blocks for almost all contemporary electronic devices. Mono-Si

serves as both a PV and light-absorbing substance for making solar cells. The silicon in the material has a crystal lattice that extends without interruption to the borders of the solid and has no grain boundaries [22-24]. Figure 3 depicts a Mono c-Si solar cell, the initial production of Solar cells.

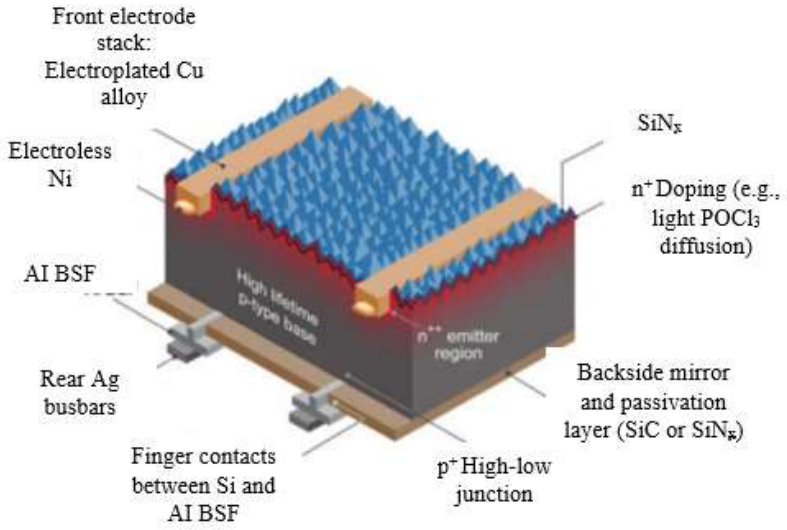

Figure 3: Structure of Mono c-Si solar cell [25-26].

Poly/Multi c-Si Solar cell

Trichlorosilane sedimentation over silicon rods is a common method for producing poly/Multi $c-Si$ solar cells at high temperatures. Distinct crystalline formations are produced during the solidification of molten silicon [27-28]. As associated with Mono $c-Si$ solar panels, polycrystalline silicon solar cells are easier and cheaper to generate due to their low processing cost; however, their efficiency is lower at 12%-14% before being improved to a maximum of 23.2% [29]. These cells alone made for around 50% of the total solar cells produced globally in 2008. The demand for these cells continues to be significant in several different countries today. This kind of cell is exemplified by ribbon Silicon. Figure 4 indicates the Multi $c-Si$ Solar cell.

Figure 4: Multi c-Si Solar cell [30]

ii. Second Generation Solar Cells-Thin Film Solar Cells

Second-generation solar cells, such as those made from a thin film and $a-Si$, are more cost-effective than their silicon wafer predecessors. Kinds of Thin-Film Solar Cells are [31]:

- $a-Si$ Thin Film

- Cd-Te Thin Film Solar Cell
- CIGS Solar Cell

a-Si Thin Film

The earliest mass-produced Solar Cells were $a-Si$ PV modules. Making $a-Si$ solar cells at a low processing temperature paves the way for their usage on a broad range of polymer, low-cost, and more flexible substrates. As compared to other substrates, these have a lower energy need for management [32]. $a-Si$ solar cells are more economically viable and widely available. The word amorphous describes the lack of a defined arrangement of atoms in the lattice, the absence of a crystalline structure, or the lack of a highly structured silicon material within a solar cell.

$a-Si$ solar cells have a main drawback in their low and erratic efficiency. At the level of the PV module, the E_{ff} of the cells automatically decreases. Commercial PV modules have an efficiency of between 4 and 8% now. They work well in climates that are constantly changing, such as those where the sun only beams for a few hours every day, and they can be easily used at higher temperatures [33].

The $p-i-n$ configuration is employed in $a-Si$ thin film solar cells. The bands are skewed due to the constructed electric field of the $p-i-n$ structure, and an inherent potential is produced when electrons are given from the n-layer to the p-layer [34]. Its $p-i-n$ form has been the subject of extensive study by a wide range of investigators [35-36]. Figure 5 indicates the diagram of $a-Si:H$ p-i-n cell.

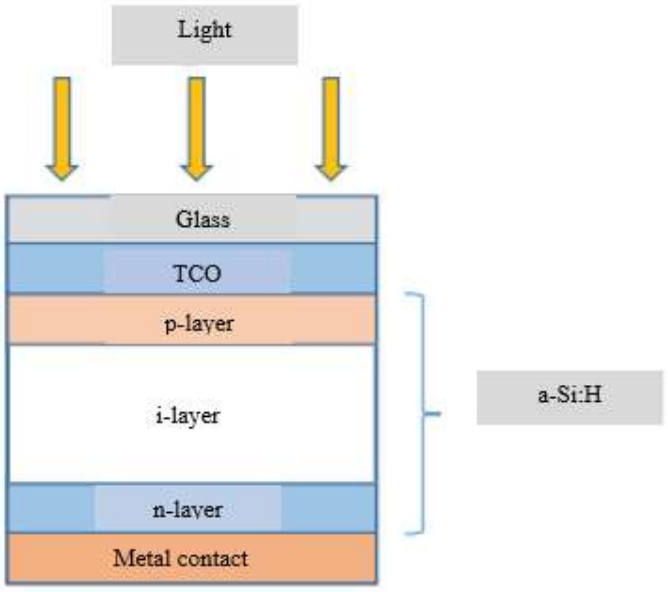

Figure 5: Diagram of $a-Si:H$ $p-i-n$ cell [37].

iii. Third Generation Solar Cells (New Emerging Technologies)

The electrical conductivity of third-generation solar cells, also called multi-junction solar cells, was greatly enhanced while still maintaining very low production costs. Several different third-

generation cell types are described below [38]:

- Nanocrystal based Solar cells
- Polymer-based Solar cells
- Dye-sensitized Solar cells
- Concentrated Solar cells [39]

2. Literature of Review

In this section, the author provides the literature review based on the efficiency and durability of thin-film p-type $a-Si:H$ solar cells

Liu et al., (2022) [40] determined the impact of light soaking on the dark conductance of boron-doped $a-Si:H$ thin films. Boron doping is triggered by the light-induced dispersion and hopping of weakly bound hydrogen atoms. As the Solar cell loses its light source, the effect reverses and the dark conductivity falls gradually. Silicon Heterojunction (SHJ) Solar cells with this effect implemented had a qualified complete area power E_{ff} of 25.18% on a 244.63 cm^2 wafer, with an FF of 85.42%.

Prayogi et al., (2022) [41] discovered that the E_{ff} of an $a-Si:H\ p-i-n\ to\ p-i_1-i_2-n$ solar cell formation was significantly improved by the addition of active layers. The $a-Si:H$ $p-i_1-i_2-n$ solar cells were produced on an Indium Tin Oxide (ITO) substrate by PECVD. The $a-Si:H\ p-i_1-i_2-n$ structure of solar cells is optimized to absorb the remaining solar energy that escapes the first intrinsic layer. Comparing the $p-i_1-i_2-n$ sample to the $p-i_1-i_2-n$ sample, they see a significant improvement from 7.79% to 8.49%.

Hamdani et al., (2022) [42] employed the Automat for Simulation of Heterostructures (AFORS-HET) program to analyze data from a $p-i-n$ solar cell that was built using a (p) $a-SiOx:H$ type active layer and an $a-Si:H$ buffer layer. The optimal dopant values of N_A = 1.0 x 1019 cm-3 and N_D = 1.0 x 1019 cm-3 were found to provide a maximum E_{ff} of 8.81% (FF = 83.85%, V_{oc} = 1042 mV, J_{sc} = 10. 08 mA/cm2) in a simulated optimized Cell B. Cell B's E_{ff} can be improved from 5.61% to 8.81% utilizing the optimal values, according to a comparison of experimental data and modeling findings.

Leila et al., (2021) [43] presented the outcomes of an $a-Si:H$ solar cell simulation run using the Analysis of Microelectronic and Photonic Structures (wxAMP 65) program. One of the principal photovoltaic uses for $a-SiC:H$ is as a p-type window layer in $a-Si$ solar cells. Authors have simulated the efficiency of a $(p)\ a-SiC:H/(i)\ a-Si:H/(n)\ a-Si:H$ heterojunction Solar cells to see whether it can help boost the implementation of a conventional $a-Si:H$ cell. Optimal initial E_{ff} for photovoltaics has been measured at 10.59% after studying the impacts of an $a-SiC:H$ window layer.

Abega et al., (2021) [44] demonstrated the use of an ITO Back Reflector Layer (BRL) to replicate ultrathin Solar cells established on $a-Si:H$. SCAPS-1D was used to calculate the outcomes of the investigation. Optimal E_{ff} of 12.71% was determined to exist at a thickness of 1 μm for the intrinsic layer. The study provided an advance toward more efficient Solar cells

based on $a-Si$ technology.

Hu et al., (2021) [45] employed PECVD to create boron-doped $Si:H$ p-layers at a substrate temperature as low as 60° C, with varying amounts of hydrogen gas (50, 100, and 150) as the reactant. These films were found to have crystalline fractions in the volume of about 16%, 52%, and 73%, respectively. Single junction $a-Si:H$ solar cells that used the Glass/TCO/$p-i-n$/Al structure had already integrated these p-layers. Preparing the p-layer with a dilution ratio of 50 using hydrogen gas was shown to be most beneficial for device performance. Energy E_{ff} of 9.0% was reached in a dot cell with an area of 0.1256 cm^2.

Chang et al., (2020) [46] performed a thorough economic comparison of n-type and p-type wafers employing a Monte Carlo simulation method, factoring in a broad range of uncertainty in manufacturing costs, wafer costs, and cell performance. It was determined that the cost gap among n-type and p-type wafers, and the cost of SHJ processing, were the three most important elements affecting the commercial difference among wafer types. Based on the results of the study, p-type SHJ solar cells should strive for a performance level that is within 0.4% of that achieved with n-type wafers. Table 1 indicates the comparison of the literature of review.

Table 1: Comparison of Literature of review.

Authors	Techniques	Outcomes
Liu et al., (2022) [40]	PECVD	Wafers with a total area of 244.63 cm2 (226.71 cm2) show a PCE of 25.18% (25.45%) and an FF of 85.42% (84.63%) due to the light-soaking impact improving the charge carrier transport in SHJ solar cells.
Prayogi et al., (2022) [41]	PECVD on ITO	An improvement in E_{ff} from 7.79% in the $p-i_1-i_2-n$ sample to 8.49% in the $p-i_1-i_2-n$ sample was achieved by studying the impact of active layer thickness on the E_{ff} of a-Si: H.
Hamdani et al., (2022) [42]	AFORS-HET	Cell B was found to have an impressive 8.81% E_{ff} (J_{sc} = 10.08 mA/cm2, V_{oc} = 1042 mV, FF = 83.85%) when dopant concentrations of N_A = 1.0 x 1019 cm-3 and N_D = 1.0 x 1019 cm^3 were used.
Leila et al., (2021) [43]	wxAMPS-1D	It was successful in achieving the impressive first E_{ff} of 10.59%.
Abega et al., (2021) [44]	SCAPS-1D	At a thickness of 1 m and a bulk defect density of 109 cm^3 of the i-layer and a surface defect density of 1010 cm^2 at the buffer layer/-($a-Si:H$) interface, the optimal structure of the ultrathin $a-Si:H$ -based Solar cell yields an E_{ff} of 12.71%.

Hu et al., (2021) [45]	PECVD	A 9.0% E_{ff} was attained by using a V_{oc} of 0.90 V, an FF of 0.65, and a J_{sc} of 15.2 mA/cm^2.
Chang et al., (2020) [46]	Monte Carlo simulation	Based on the results of the study, p-type SHJ solar cells should strive for a performance level that is within 0.4% of that achieved with n-type wafers.

3. Background study

In the work, thin films of $a-Si{:}H$ were accumulated using PECVD, analyzed, synthesized, and characterized. There were three different film kinds placed. The initial series (00 procedure) saw the doping of an inherent $a-Si{:}H$ film. n-type samples were doped in the second series (A1-A5 procedure) using a gas combination of dihydrogen (H_2), silane (SiH_4), and phosphine (PH_3). SiH_4, H_2, and B_2H_6 were used to dope p-type samples in the third series (B1-B5 procedure). AFM was utilized to evaluate the surface morphology of the films, while Scanning Electron Microscopy (SEM) was employed to analyze the films, and ultraviolet-visible ellipsometry was utilized to determine the optical band gap and film thickness. The conductivity graphs show that films with the largest dopant gas flow (phosphine or diborane) had the maximum conductivities, contrasted to the least necessary for materials built of $a-Si{:}H$ silicon for high-quality Solar cells. An improvement in conductivity of many orders of magnitude is a promising finding that might lead to more efficient Solar cells based on $a-Si{:}H$, as demonstrated by the data [47].

4. Problem Formulation

PECVD which was utilized to dope the $a-Si{:}H$ film series. The sequence's p-type films were doped with SiH_4, H_2, and B_2H_6 mixes (B1–B6 method). The specimens in the collection were all manufactured of glass (Corning Glass 2974 and 1737). The study was done using the AMP-3300 Plasma II PECVD Deposition System. Series B1-B5 was deposited for 30 minutes at a constant 300 W of power, 600 $mTorr$ of pressure, 90 mW/cm^2 of power density, and 300 C temperature. Authors were able to satisfy numerous criteria by altering the H_2, SiH_4, and PH_3 gas series flows. The p-layer deposition process has five unique versions, which are denoted by the letters B1 through B5. Throughout PECVD tests, authors kept the p-layer growth rate constant at 50 $sccm$ of silane gas and the chamber pressure in 2000 $mTorr$. A dilution ratio of 1000 $sccm$ of hydrogen was employed to create the p-layers in layers B2-B5, whereas the first p-layer had a dilute ratio of 200 $sccm$.

5. Research Objectives

i. While having a relatively low industry-maximum efficiency, its high absorption capacity allows it to be employed in solar cells with very small layer thicknesses (typically approximately a factor of 100 less than in crystalline silicon).

ii. Using fewer Eg defects, electrons in the valence band could be driven to the conduction band, improving carrier strength, electrical conductivity using Hydrogen atoms technology linked to empty Si bonds lower bandgap energy defect.

iii. To integrate fiberglass noise reduction barriers with solar cells by optimizing films, p-i-n junction characteristics, and solar cell design/geometry (top contact grid parameters).

6. Material and methods

In the section, one type of film was deposited. The PECVD process was used to dope the set off $a-Si{:}H$ films. The p-type films in the series were doped with a combination of SiH_4, H_2, and B_2H_6 (B1–B6 method). Glass models were used in the series (Corning Glass 1737 and 2974). The AMP-3300 Plasma II PECVD Deposition System was utilized. The invariant deposition settings for series B were 600 $mTorr$ ambient pressure, 300 W power, 90 mW/cm^2 power density, and 30 min treatment time. The flows of H_2, SiH_4, and PH_3 gases in the series were changed to meet certain conditions, as stated in Table 2. The flow rates of SiH_4 and PH_3 gases were adjusted to 50 as well as 0 $sccm$, correspondingly. The hydrogen dilution procedure was carried out for the p-layer at constant flow rates of 100 and 200 $sccm$, respectively.

Table 2: Gas flows of H_2, SiH_4, PH_3 and B_2H_6 series

Process	$\boldsymbol{H_2}$ $\boldsymbol{(sccm)}$	$\boldsymbol{SiH_4}$ $\boldsymbol{(sccm)}$	$\boldsymbol{PH_3}$ $\boldsymbol{(sccm)}$	$\boldsymbol{B_2H_6}$ $\boldsymbol{(sccm)}$
B1	200	50	0	4
B2	1000	50	0	5
B3	1000	50	0	6
B4	1000	50	0	8
B5	1000	50	0	10

The p-layer deposition method has been divided into B1-B5 variants. The vacuum in the PECVD chamber was adjusted to 2000 $mTorr$, and the silane gas utilized for p-layer formation was tuned to a continuous variable of 50 $sccm$. The initial p-layer was developed with a hydrogen dilution ratio of 200 $sccm$, whereas the p-layers from B2-B5 were produced with a hydrogen dilution ratio of 1000 $sccm$.

6.1 Single p-i-n Junction Fabrication

Figure 6 depicts the accumulation method schematic in the PECVD. During the accumulation period, the p-layer was accumulated on the initial chamber. The substrate was then moved to a different chamber for the i-layer depositing procedure. The i-layer deposition method was performed independently from the extrinsic procedure to avoid contamination of dopant gases, which could affect silicon impurity.

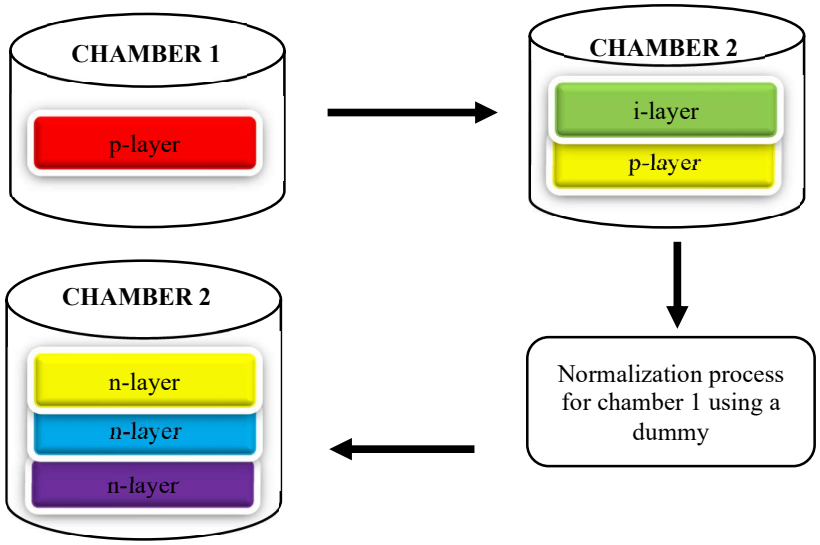

Figure 6: Manufacture method of Solar cell inside PECVD chamber

The substrate was not returned to the first chamber immediately after the i-layer deposition procedure was completed. The substrate was held constant within chamber 2 without any gas flow, although the fake sample was utilized to normalize the initial chamber by showing it with nitrogen gas. The chamber 1 normalization procedure is required to ensure that the n-layer removal method is free of p-layer dopant gas contamination.

7. Results

In this section of results, the author finds a result based on layer characteristics, solar cell performance, and optimization of layer thickness.

7.1 Layer Characteristics

The physical parameters of each fabrication process (B1-B5) have been determined. AFM was used to measure process thicknesses. The thicknesses acquired are utilized to calculate the deposition rate of each operation. Table 3 shows the Solar cell deposition parameters for each procedure.

Table 3: Solar cell deposition parameter for each process

Process	RH_2/SiH_4	Deposition Rate (nm/s)	Time (min)	Thickness (nm)	Energy Gap (Eg) (eV)
B1	2	0.072	15	43	2.0
B2	0	0.028	236	400	1.9
B3	16	0.012	570	400	1.6
B4	36	0.042	160	400	1.4

B5	1	0.120	15	36	2.2

The B1 in an $a-Si{:}H$ solar cell has an Eg of 2.0 eV. The p-layer was divided into five processes, yielding Eg of 2.0 eV, 1.9 eV, 1.6 eV, 1.4 eV, and 2.2 eV for hydrogen ratios of 2, 0, 16, 36, and 1. The reduction of the Eg is generated by a hydrogen atom, which causes separation by improving ion/electron collisions and influences energy from the expanding surface by filling vacancies in the gap. A different aspect that contributes to the reducing Eg is the potential of increased crystallization degree, which is evident at high-level hydrogen reduction ratios.

Thickness is a crucial aspect of the fabrication process. The thickness of B1 and B2-B4 was reduced so that incoming photons are not absorbed as much. B5 is mostly used as a photon filler that absorbs photons when needed. In the work, the p-layer was grown thicker to improve photon absorption.

7.2 Solar Cell Performances

Table 4 demonstrates how the E_{ff} performing of a Solar cell is impacted by the player Eg. After the p-layer Eg is adjusted from 2.0 eV to 2.2 eV, the J_{sc} and cell efficiency rise by around 0.0147 A/m2 and 0.75%, respectively. The graph also demonstrates a 0.24% decline in cell efficiency, as evidenced by a fall in J_{sc}.

Table 4: Sample structure and cell performance

Process	$\boldsymbol{J_{sc}}$ **(A/m^2)×10^{-2}**	$\boldsymbol{V_{oc}}$ **(V)**	$\boldsymbol{FF}$ **(%)**	**Efficiency ($\boldsymbol{E_{ff}}$)**
B1	2.65	0.214	40.4	4.86
B2	4.12	0.163	41.1	5.61
B3	4.04	0.159	39.7	5.37
B4	3.14	0.154	34.9	4.83
B5	4.10	0.144	32.4	4.53

The peak of the sun's rays falls between 1.4 and 2.2 eV in energy, which corresponds to the red and green ends of the visible spectrum, as seen by the solar flux distribution. A greater variety of photons from the sun's spectrum is received by Solar cells and converted into usable energy. In terms of efficiency, Solar cells with a p-layer Eg between 1.9 and 1.6 eV seem to outperform those with a p-layer Eg of 2.2 eV due to the influence of photon dispersion.

Compared to the alternative process, the V_{oc} of the sample, B1 is much higher. Table 4 demonstrates that the V_{oc} drops with the hydrogen dilution ratio. The existence of a hydrogen atom during the accumulation process can raise the dispersion coefficient on a growing surface, resulting in the formation of a crystalline phase seed on the layer. It could create a more durable thin layer and has a high carrying flexibility as the hydrogen ratio increases.

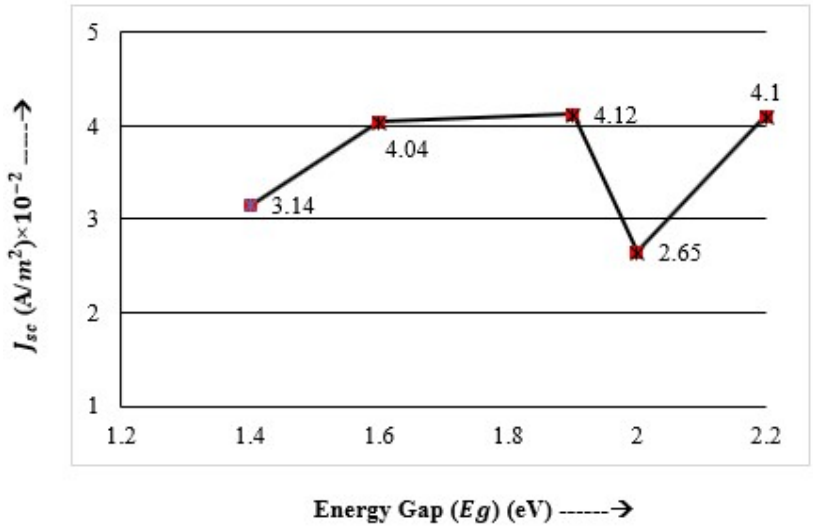
5
4
3
2
1
1.2
1.4
1.6
1.8
2
2.2
3.14
4.04
4.12
2.65
4.1
J_{sc} (A/m^2)×10^{-2} ----→
Energy Gap (Eg) (eV) ------→

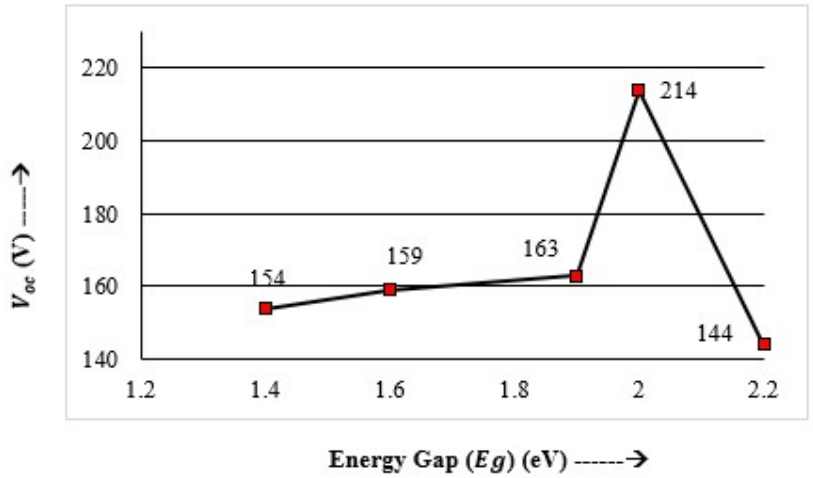
220
200
180
160
140
1.2
1.4
1.6
1.8
2
2.2
154
159
163
214
144
V_{oc} (V) ----→
Energy Gap (Eg) (eV) ------→

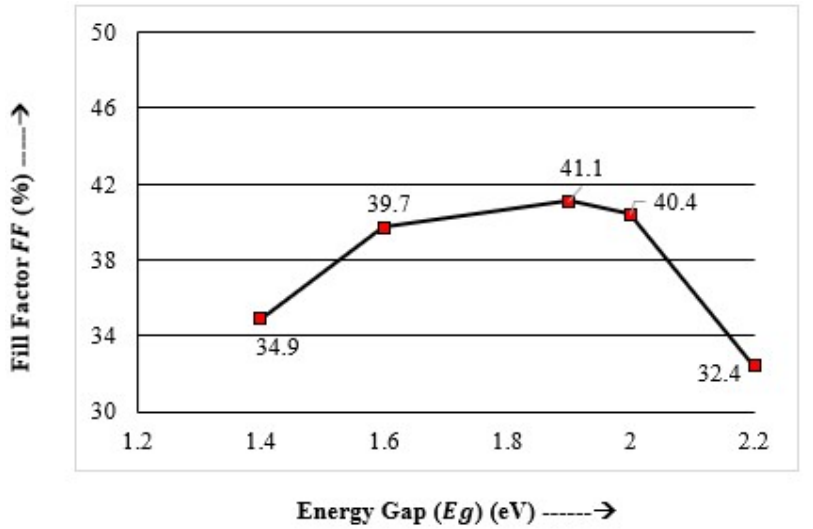
50
46
42
38
34
30
1.2
1.4
1.6
1.8
2
2.2
34.9
39.7
41.1
40.4
32.4
Fill Factor FF (%) ----→
Energy Gap (Eg) (eV) ------→

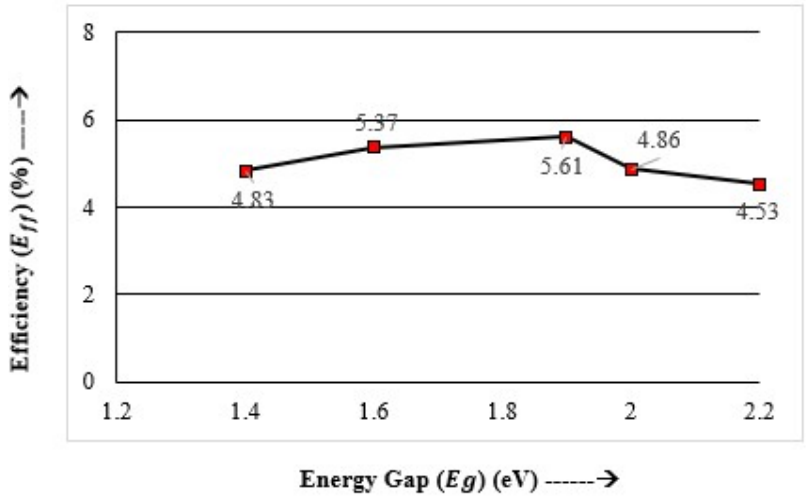

Figure 7: Solar cell E_{ff} based on p-layer Eg

The performing graph of the B1-B2 Solar cell efficiency versus the p-layer Eg is shown in Figure 7. Sample B1 achieved an FF of 40.4% and an E_{ff} of 4.86%. Sample B2 achieved an FF of 41.4% and an E_{ff} of 5.61%. Sample B3 had an FF of 39.7 and an E_{ff} of 5.37%, whereas Sample B4 had an FF of 34.9% and an E_{ff} of 4.83%. FF was 32.4% and E_{ff} was 4.53% for sample B5. Gains in effectiveness were seen in the energy ranges of 1.6 eV and 1.9 eV. The 2.2 eV Eg was the location of the performance drop. As a result, the energy from absorbed photons is not used effectively.

Photons with an Eg larger than 1.4 eV are one of the factors contributing to poor E_{ff}. Higher energy photons than those in the p-layer would be absorbed, moving the electrons from the valence band to the conduction band and putting away a hole in the valence band. The electron-hole pair swiftly relaxes back on the band's edge after releasing heat energy.

The hydrogen dilution ratio during the deposition procedure is one of the elements that impact Solar cell performance. The Solar cell's efficiency can be increased using B2. The results from the hydrogen atom's attachment to the Si atom's reactive free electron. The bandgap energy defect would decrease when a hydrogen atom is bound to an unfilled Si bond. The electrons in the valence band could be further readily stimulated to the conduction band with fewer defects in the Eg, which would improve carrier strength, increase electrical conductivity, and increase E_{ff}.

7.3 Optimization of Layer Thickness

Given that the p-layer is the primary absorber layer, the thickness of the p-layer is a factor that could have a substantial influence on the performance of the Solar cell. The creation of electron-hole pairs would grow as the p-layer thickness improves because more photon energy would be absorbed. Samples B1 through B5 that have undergone the optimization outlined above differ in terms of their p-layer thickness, as indicated in Table 5. Sample B1 produced results of 5.61% E_{ff} and 41.1% FF with a p-layer thickness of 400 nm. Sample B2 produced 5.69% E_{ff} and 41.6% FF with a 500 nm p-layer thickness. 5.78% E_{ff} and 42.6% FF were obtained for Sample B3 with a 600 nm p-layer thickness, while 5.88% E_{ff} and 43.4% FF were

obtained for Sample B4 with a 700 nm p-layer thickness. Nevertheless, Sample B5's 800 nm p-layer thickness produced a 5.91% E_{ff} and a 43.8% FF.

Table 5: Sample structure and cell performance.

Process	p-layer Thickness (nm)	J_{sc} (A/m^2) ×10^{-2}	V_{oc} (V)	FF (%)	E_{ff} (%)
B1	400	4.12	0.163	41.1	5.61
B2	500	6.05	0.251	41.6	5.69
B3	600	5.13	0.277	42.6	5.78
B4	700	4.03	0.285	43.4	5.88
B5	800	5.18	0.346	43.8	5.91

The improvement in cell performance shown in Figure 8 occurs after the p-layer thickness has been increased by 400 nm to 800 nm.

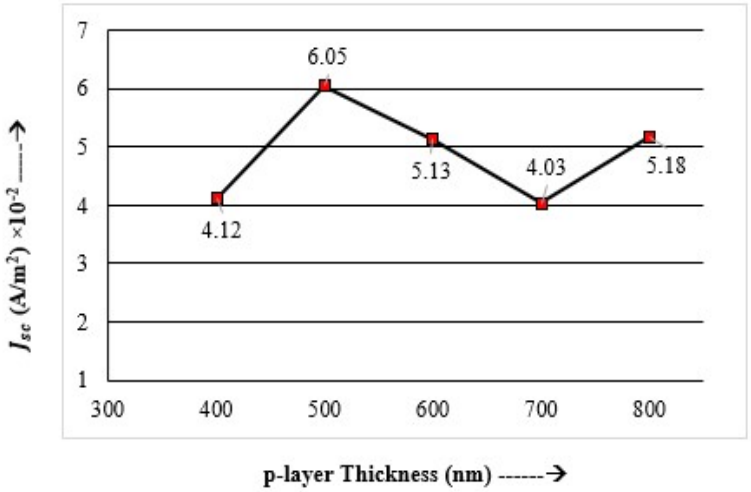

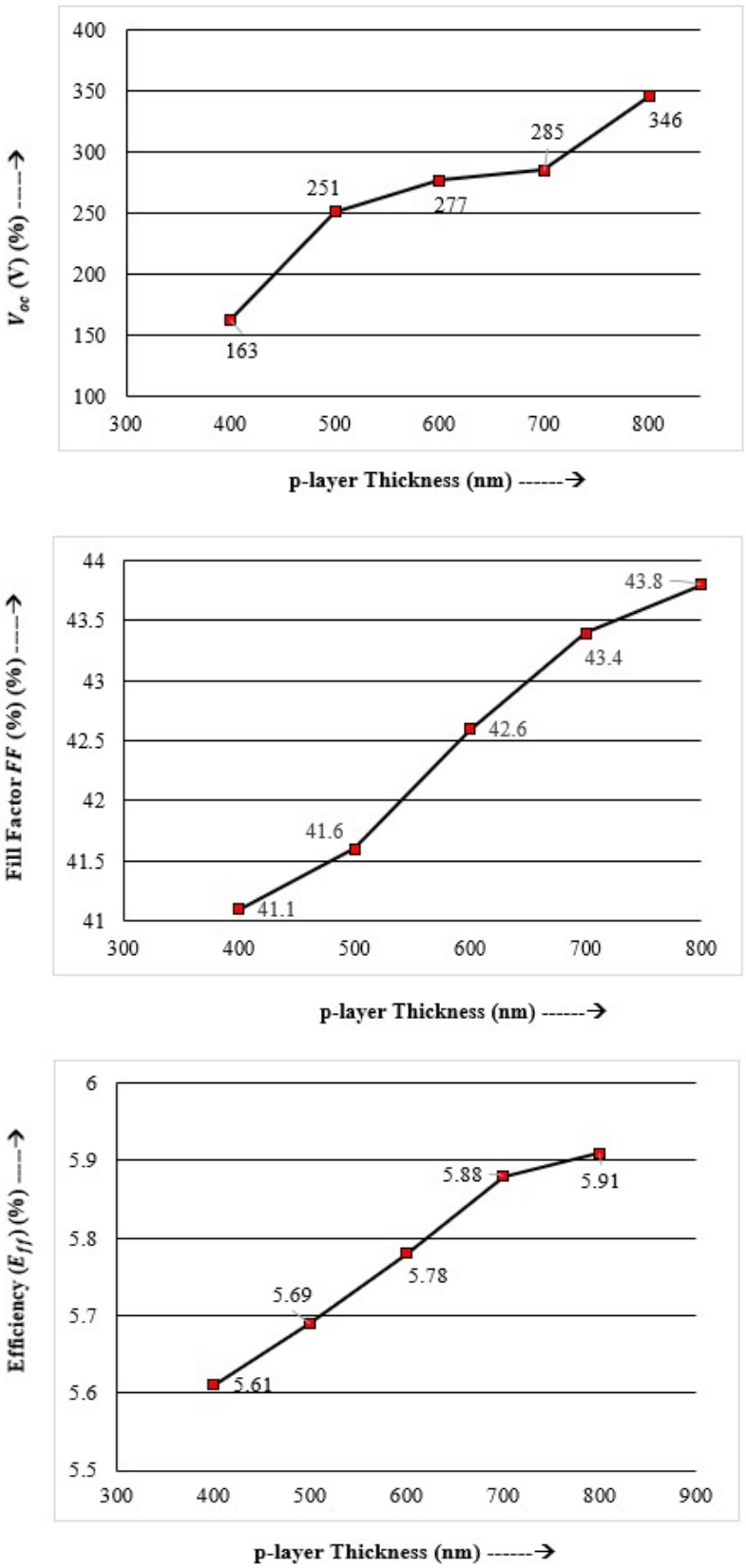

Figure 8: Enhancing performance by adjusting p-layer thickness

The expansion of the depletion area is something that leads to an improvement in Solar cell performance and an accompanying rise in p-layer thickness. The depletion area would widen as a result of the thicker p-layer, allowing for the growth of donor and acceptor ions such as electrons and holes. Additionally, the dilatation of the reduction area induces an increase in ion diffusion length, which increases lifespan and drift currents.

8. Conclusion

It is anticipated that the $a-Si:H$ alloy would perform a main role in boosting the E_{ff} and consistency of $a-Si:H$ solar cells. Here, authors use AFM to quantify the thicknesses of several processes and do simulations on how they can affect the efficiency of Solar cells based on $a-Si:H$ grown by PECVD. Changing the hydrogen gas ratio reduces the p-layer Eg from 2.2 eV to 1.4 eV. Solar cell E_{ff} is mostly defined by the p- layer's Eg. Increasing the p-layer Eg from 1.4 eV to 2.2 eV yielded Solar cell E_{ff} of 4.86%, 5.61%, 5.37%, 4.83%, and 4.5% in the study. Increasing p-layer thickness can extend the reduction region in Solar cells' p-n junction region. E_{ff} improvements of 5.61% at 400 nm, 5.69% at 500 nm, and 5.78% at 600 nm. A Solar cell made out of $a-Si:H$ achieved a peak E_{ff} of 5.91% with an p-layer Eg of 2.2 eV and a thickness of 800 nm.

Reference

1. https://ocw.tudelft.nl/wp-content/uploads/Solar-Cells-R5 CH7_Thin_film_Si_solar_cells.pdf.
2. Corpus Mendoza, Asiel Neftali. "Influence of the p-type layer on the performance and stability of thin film silicon solar cells." Ph.D. diss., University of Sheffield, 2017.
3. H. Schade, Module fabrication and performance, in A. Shah (Ed.), Thin-Film Solar Cells, EPFL Press, Switzerland, 2010, pp. 311–315.
4. Belfar, Abbas, and Wafa Hadj Kouider. "Improvement in a-Si: H silicon solar cells with using double p-type window layers based on nanocrystalline silicon oxide." Optik 244 (2021): 167610.
5. Yadav, A. and Kumar, P. (2015) Enhancement in Efficiency of PV Cell through P&O Algorithm. International Journal for Technological Research in Engineering, 2, 2642-2644.
6. Castellano, R. (2010) Solar Panel Processing. Old City Publishing Inc., Philadelphia.
7. Tripathi, SumanLata, Sobhit Saxena, and Sushmita Kumari. "A Review on Design and Performance Evaluation of Solar Cells and Panels." Think India Journal 22, no. 17 (2019): 2786-2796.
8. Srinivas, B., Balaji, S., Nagendra Babu, M. and Reddy, Y.S. (2015) Review on Present and Advance Materials for Solar Cells. International Journal of Engineering Research-Online, 3, 178-182.
9. McEvoy, A., Castaner, L. and Markvart, T. (2012) Solar Cells: Materials, Manufacture, and Operation. 2nd Edition, Elsevier Ltd., Oxford, 3-25.

10. (2015-2016) Energy from the Sun, Student Guide. National Energy Education Development Project (NEED).

11. Grisham, L.R. (2008) Nuclear Fusion in Future Energy, Improved, Sustainable and Clean Options for our Planet, Edited by Trevor M. Letcher, 2nd Edition, Elsevier Ltd., Amsterdam, 291-301.

12. Fahrenbruch, A.L. and Bube, R.H. (1983) Fundamentals of Solar Cells. Academic Press Inc., New York.

13. Bertolli, M. (2008) Solar Cell Materials. Course: Solid State II. Department of Physics, University of Tennessee, Knoxville.

14. Bagher, A.M., Vahid, M.M.A. and Mohsen, M. (2015) Types of Solar Cells and Application. American Journal of Optics and Photonics, 3, 94-113.

15. Liang Huang, Huixu Deng, Thach Pham, Matthew Young, Hameed Naseem, HusamHamzaAbuSafe, Xiaodong Yang, Shui-Qing Yu, "Amorphous Silicon Solar Cells Using Metallic Fishnet Nanostructures Simultaneously for Schottky Contact and Plasmonics Enhancement‖ IEEE Photovoltaic Specialists Conference (PVSC), pp.1353-1356, 2013

16. RabinaBhujel and Bibhu P. Swain, ―Fabrication and characterization of silicon nanowires hybrid Solar cells: A Review‖, International Conference on Mechanical, Materials and Renewable Energy, vol.377(1757-899X), pp.1- 19,2018.

17. Du John H, Victor, Jacquline Moni D, and D. Gracia. "A detailed review on Si, GaAs, and CIGS/CdTe based solar cells and efficiency comparison." Przegląd Elektrotechniczny 96 (2020).

18. Choubey, P.C., Oudhia, A. and Dewangan, R. (2012) A Review: Solar Cell Current Scenario and Future Trends. Recent Research in Science and Technology, 4, 99-101.

19. Sharma, Shruti, Kamlesh Kumar Jain, and Ashutosh Sharma. "Solar cells: in research and applications—a review." Materials Sciences and Applications 6, no. 12 (2015): 1145.

20. Srinivas B Balaji S Babu M N and Reddy Y S, ―Emerging Nanostructure material for energy and environmental Scienec‖ J. Eng. Res., vol.3, pp.178, 2015.

21. Mohammad TawheedKibria, AkilAhammed, Saad Mahmud Sony, Faisal Hossain, Shams-Ul-Islam, ―A Review: Comparative studies on different generation solar cells technology‖ International Conference on Environmental Aspects of Bangladesh, ICEAB, pp.51-53, 2014.

22. Wurfel, P. and Wurfel, U. (2009) Physics of Solar Cells: From Basic Principles to Advanced Concepts. John Wiley & Sons, Hoboken.

23. Dmitrijev, S. (2006) Principles of Semiconductor Devices. Oxford University Press, Oxford.

24. Bagher, Askari Mohammad, Mirzaei Mahmoud Abadi Vahid, and Mirhabibi Mohsen. "Types of solar cells and application." American Journal of optics and Photonics 3, no. 5 (2015): 94-113.

25. Goodrich A, Hacke P, Wang Q, Sopori B, Margolis R, James TL. A wafer-based monocrystalline silicon photovoltaics road map: utilizing known technology improvement opportunities for further reductions in manufacturing costs. Sol Energy Mater Sol Cells 2013; 114:110–35.

26. Kutraleeswaran, M., M. Venkatachalam, M. Saroja, P. Gowthaman, and S. Shankar. "Dye-sensitized Solar Cells, —A Review." J. Adv. Res. Appl. Sci 4 (2017): 26-38.

27. Jiang, L., Cui, S., Sun, P., Wang, Y., & Yang, C. 2020. Comparison of Monocrystalline and Polycrystalline Solar Modules. Proceedings of 5th IEEE Information Technology and Mechatronics Engineering Conference: 341- 344, https://doi.org/10.1109/ITOEC49072.2020.9141722.

28. Fujiwara, K., Pan, W., Usami, N., Sawada, K., Tokairin, M., Nose, Y., Nomura, A., Shishido, T., & Nakajima, K. 2016. Growth of structure-controlled polycrystalline silicon ingots for solar cells by casting. Acta Materialia. 54(12): 3191-3197, https://doi.org/10.1016/j.actamat.2006.03.014.

29. Sharma, S., Jain, K.K., & Sharma, A.2015.Solar Cells: In Research and Applications-A Review. Mater. Sci. and Appl. 6: 1145-1155, https://doi.org/10.4236/msa.2015.612113.

30. Di Vece, Marcel. "Using nanoparticles as a bottom-up approach to increase solar cell efficiency." KONA Powder and Particle Journal 36 (2019): 72-87.

31. Durganjali, C. Santhi, Sameer Bethanabhotla, Satwik Kasina, and Sudha Radhika. "Recent developments and future advancements in solar panels technology." In Journal of Physics: Conference Series, vol. 1495, no. 1, p. 012018. IOP Publishing, 2020.

32. Imamzai, M., Aghaei, M., Hanum Md Thayoob, Y. and Forouzanfar, M. (2012) A Review on Comparison between Traditional Silicon Solar Cells and Thin-Film CdTe Solar Cells. Proceedings of National Graduate Conference (NatGrad 2012), Tenaga Nasional Universiti, Putrajaya Campus, 8-10 November 2012, 1-5.

33. Maehlum, M.A. (2015) Energy Informative The Homeowner's Guide To Solar Panels, Best Thin Film Solar Panels— Amorphous, Cadmium Telluride or CIGS? Last updated 6 April 2015.

34. K. W. Böer, Handbook of the Physics of Thin-Film Solar Cells. Springer Science & Business, 2014

35. C.-M. Yang, Y.-H. Liao, C.-H. Chen, T.-C. Chen, C.-S. Lai, and D. G. Pijanowska, "P-i-n amorphous silicon for thin-film light-addressable potentiometric sensors," Sensors and Actuators B: Chemical, pp. –, 2016

36. Y. Y. Cheng, B. Fückel, R. W. MacQueen, T. Khoury, R. G. Clady, T. F. Schulze, N. Ekins-Daukes, M. J. Crossley, B. Stannowski, K. Lips, et al., "Improving the light-

harvesting of amorphous silicon solar cells with photochemical upconversion," Energy & Environmental Science, vol. 5, no. 5, pp. 6953–6959, 2012.

37. Sarkar, Md Nazmul Islam, and Himangshu Ranjan Ghosh. "Efficiency improvement of amorphous silicon single junction solar cell by design optimization." In 2017 International Conference on Electrical, Computer and Communication Engineering (ECCE), pp. 670-675. IEEE, 2017.

38. Sharma, Divya, Rajesh Mehra, and Balwinder Raj. "Design and Analysis of Various Solar Cell Technologies for Improvements in Efficiencies: A Review." (2021).

39. Raut, Kiran H., Himani N. Chopde, and Dinesh W. Deshmukh. "A review on comparative studies of diverse generation in the solar cell." Int. J. Electr. Eng. Ethics 1 (2018): 1-9.

40. Liu, Wenzhu, Jianhua Shi, Liping Zhang, Anjun Han, Shenglei Huang, Xiaodong Li, Jun Peng, et al. "Light-induced activation of boron doping in hydrogenated amorphous silicon for over 25% efficiency silicon solar cells." Nature Energy 7, no. 5 (2022): 427-437.

41. Prayogi, Soni, Yoyok Cahyono, and Dadan Hamdani. "Effect of active layer thickness on the performance of amorphous hydrogenated silicon solar cells." Engineering and Applied Science Research 49, no. 2 (2022): 201-208.

42. Hamdani, Dadan, Soni Prayogi, Yoyok Cahyono, Gatut Yudoyono, and Darminto Darminto. "The effects of dopant concentration on the performances of the a-SiOx: H (p)/a-Si: H (i1)/a-Si: H (i2)/μc-Si: H (n) heterojunction solar cell." International Journal of Renewable Energy Development 11, no. 1 (2022): 173.

43. Leila, Ayat, Meftah Afek, Idda Ahmed, and Zebri Halima. "Analysis and Optimization of the Performance of Hydrogenated Amorphous Silicon Solar Cell." Journal of New Materials for Electrochemical Systems 24, no. 3 (2021).

44. Abega, FX Abomo, A. Teyou Ngoupo, and J. M. B. Ndjaka. "Numerical design of the ultrathin hydrogenated amorphous silicon-based solar cell." International Journal of Photoenergy 2021 (2021): 1-13.

45. Hu, Zhihua, Shurong Wang, and Zhaohui Yao. "Low-Temperature Deposition of Boron Doped P-type Si: H Window Layers for Amorphous Silicon Solar Cells." INTERNATIONAL JOURNAL OF ELECTROCHEMICAL SCIENCE 16, no. 6 (2021).

46. Chang, Nathan L., Matthew Wright, Renate Egan, and Brett Hallam. "The technical and economic viability of replacing n-type with p-type wafers for silicon heterojunction solar cells." Cell Reports Physical Science 1, no. 6 (2020): 100069.

47. Garcia-Barrientos, Abel, Jose Luis Bernal-Ponce, Jairo Plaza-Castillo, Alberto Cuevas-Salgado, Ariosto Medina-Flores, María Silvia Garcia-Monterrosas, and Alfonso Torres-Jacome. "Analysis, Synthesis, and Characterization of Thin Films of a-Si: H (n-type and p-type) Deposited by PECVD for Solar Cell Applications." Materials 14, no. 21 (2021): 6349.